**Supporting Information**

**Propentdyopent: The scaffold of a heme metabolite as an electron reservoir in transition metal complexes**

**Contents**

***Materials and Methods.*** The propentdyopent methanol adduct was prepared as previously reported.[1,2,3] Acetonitrile (CH$_3$CN), dimethylformamide (DMF), tetrahydrofuran (THF), and dichloromethane (CH$_2$Cl$_2$) were dried by passage through a solvent purifier. Methanol (MeOH) was freshly distilled from CaH$_2$. All other reagents were obtained commercially and used as received. $^1$H NMR and $^{13}$C NMR spectra were recorded at the University of Arizona NMR Facility on Bruker DRX−600, DRX−500 or AVIII-400 instruments and calibrated using residual undeuterated solvent as an internal reference. Low- and high-resolution mass spectra were acquired at the University of Arizona Mass Spectrometry Facility. Elemental analyses were performed by Numega Resonance Labs, San Diego, CA.  UV/visible spectra were recorded on an Agilent 8453 UV/Vis spectrophotometer.

***Synthesis of Zn(pdp)₂.*** The zinc complex was prepared by slight modification of a previously reported procedure.[3] Briefly, methanol adduct Hpdp•MeOH (15 mg, 0.047 mmol) was dissolved in MeOH (10 mL) and Zn(OAc)$_2$ (5.2 mg, 0.024 mmol) added.   The reaction mixture was refluxed for 30 min and allowed to cool to room temperature. The reaction progress was monitored by UV-vis absorption spectroscopy.  Upon completion, water was added until the complex precipitated (2-3 mL).  The orange slurry was then transferred to a centrifuge tube, spun down and the supernatant was removed.  The solid was washed three times with water and dried under vacuum over CaCl$_2$ overnight.  Recrystallization from benzene gave a crystalline orange solid (21.3 mg, 71%). $^1$H NMR (600 MHz, CDCl$_3$) δ 5.71 (s, 1H), 2.50 (q, J = 7.6 Hz, 4H), 2.32 (q, J = 7.6 Hz, 4H), 1.21 (t, J = 7.6 Hz, 6H), 1.08 (t, J = 7.6 Hz, 6H). HRMS-ESI$^+$ (*m/z*): [M+H]$^+$ calcd for [C$_{34}$H$_{43}$N$_4$O$_4$Zn], 635.2576; found, 635.2570. Anal. Calcd. for [C$_{34}$H$_{42}$N$_4$O$_4$Zn]: C, 64.2; H, 6.7; N, 8.8%; found: C, 64.6; H, 7.0; N, 8.5%.

***Synthesis of Cu(pdp)₂.*** Hpdp•MeOH (15 mg, 0.047 mmol) was dissolved in MeOH (10 mL) and Cu(OAc)$_2$ (0.5 equiv.) was added.   The reaction mixture was refluxed for 20 min and allowed to cool to room temperature. Evaporation of the solvent under reduced pressure gave a brown powder.  CH$_2$Cl$_2$ was added and the mixture was filtered through Celite to remove any unreacted metal salt.  The filtrate was evaporated and the resulting solid was further purified by crystallization. Slow evaporation from CHCl$_3$ at 4 °C (5 mg/0.5 mL) gave the desired products as a crystalline red solid (14.6 mg, 49%). HRMS-ESI$^+$ (*m/z*): [M+H]$^+$ calcd for C$_{34}$H$_{43}$N$_4$O$_4$Cu, 634.2580; found, 634.2575. Anal. Calcd. for C$_{34}$H$_{42}$N$_4$O$_4$Cu: C, 64.2; H, 6.7; N, 8.8%; found: C, 64.8; H, 6.3; N, 9.0%.

***Synthesis of Ni(pdp)₂.*** Hpdp•MeOH (15 mg, 0.047 mmol) was dissolved in CH$_3$CN (10 mL) and NiCl$_2$ (0.5 equiv.) was added. The reaction mixture was refluxed for 30 min and formation of a red precipitate was observed. The reaction mixture was then concentrated (to 2−3 mL) and a burgundy red powder was collected on a fritted filter. This product was redissolved in CHCl$_3$ (or CDCl$_3$) and filtered through Celite. The complex was then crystallized by slow diffusion of benzene in this solution at 4 °C (19.5 mg, 65%). $^1$H NMR (600 MHz, CDCl$_3$) δ 15.22 (s, 8H), 9.18 (s, 8H), 3.22 (s, 12H), −2.26 (s, 12H), −52.70 (s, 2H)**.** HRMS-ESI$^+$ (*m/z*): [M+H]$^+$ calcd for [C$_{34}$H$_{43}$N$_4$O$_4$Ni], 629.2638; found, 629.2632. Anal. Calcd. for C$_{34}$H$_{42}$N$_4$O$_4$Ni•2H$_2$O•CDCl$_3$: C, 53.5; H, 6.3; N, 7.1%; found: C, 53.1; H, 6.8; N, 6.8%.

***Synthesis of Co(pdp)₂.*** Hpdp•MeOH (15 mg, 0.047 mmol) was dissolved in MeOH (10 mL) and CoCl$_2$ (0.5 equiv.) was added. The reaction mixture was refluxed for 20 min and allowed to cool to room temperature. Evaporation of the solvent under reduced pressure gave a brown powder.  CH$_2$Cl$_2$ was added and the mixture was filtered through Celite to remove any unreacted metal salt.   The filtrate was

evaporated, and the complex was then crystallized by slow diffusion of benzene in a solution in $CH_2Cl_2$ at 4 °C (12.2 mg, 41%). HRMS-ESI$^+$ (*m/z*): [M+H]$^+$ calcd for [$C_{34}H_{43}N_4O_4Co$], 630.2616; found, 630.2611. Anal. Calcd. for $C_{34}H_{42}N_4O_4Co \cdot H_2O \cdot C_6H_6$: C, 66.2; H, 6.9; N, 7.7%; found: C, 65.9; H, 6.4; N, 7.7%.
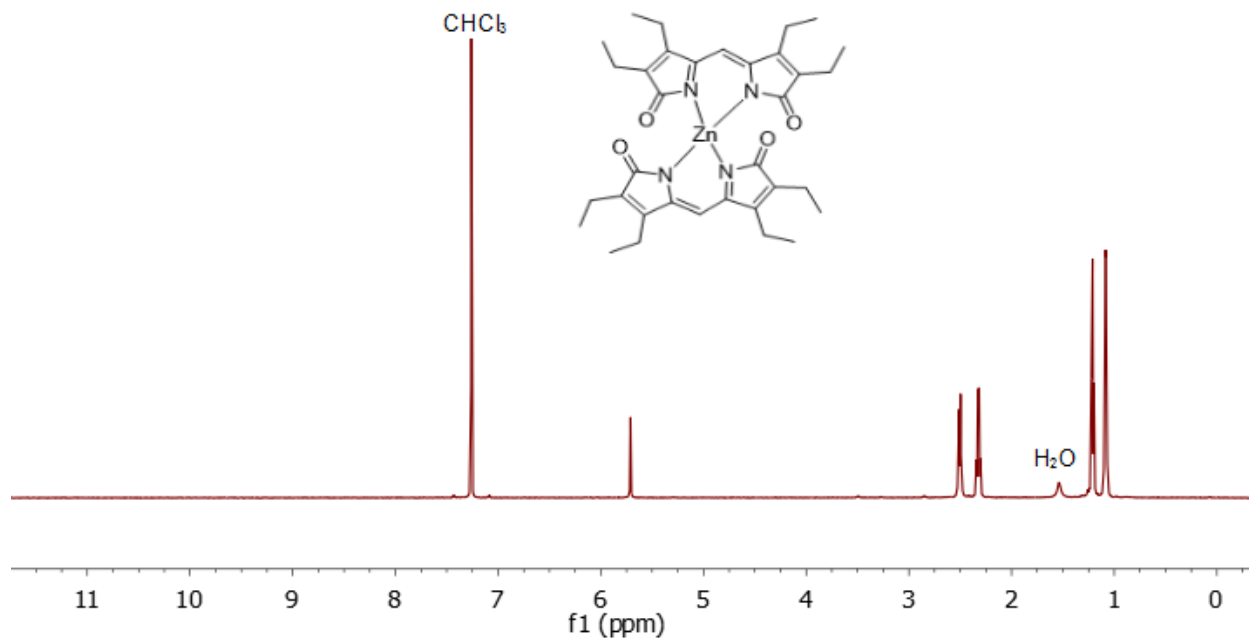


**Figure S1.** $^1H$ NMR spectra of complex Zn(pdp)$_2$ (500 MHz, CDCl$_3$, 27 °C).
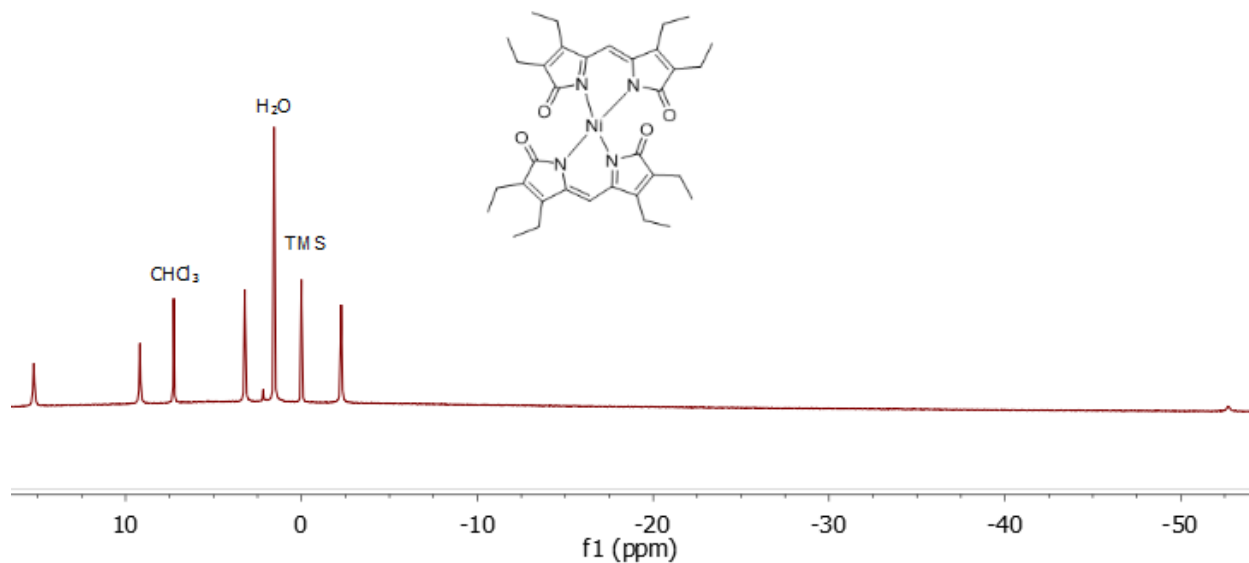


**Figure S2.** $^1H$ NMR spectra of complex Ni(pdp)$_2$ (500 MHz, CDCl$_3$, 27 °C).

**Table S1.** UV-visible absorption properties of propentdyopent complexes

| Complex | $\lambda_{max}$ ($\varepsilon$) / nm ($M^{-1}cm^{-1}$) | Solvent | Ref. |
|---------|-----------------------------------------------|---------|------|
| **Zn(pdp)₂** | 361 (26,600), 491 (26,600) and 522 (22,100) | $CH_2Cl_2$ | this work |
| **Cu(pdp)₂** | 346 (13,000), 496 (4,500), 622 (4,000) | $CH_2Cl_2$ | 4 |
| **Ni(pdp)₂** | 369 (31300), 471 (21500) | $CH_2Cl_2$ | this work |
| **Co(pdp)₂** | 368 (4,100), 464 (2,900), 548 sh (1,100), 662 (450) | $CH_2Cl_2$ | 5 |
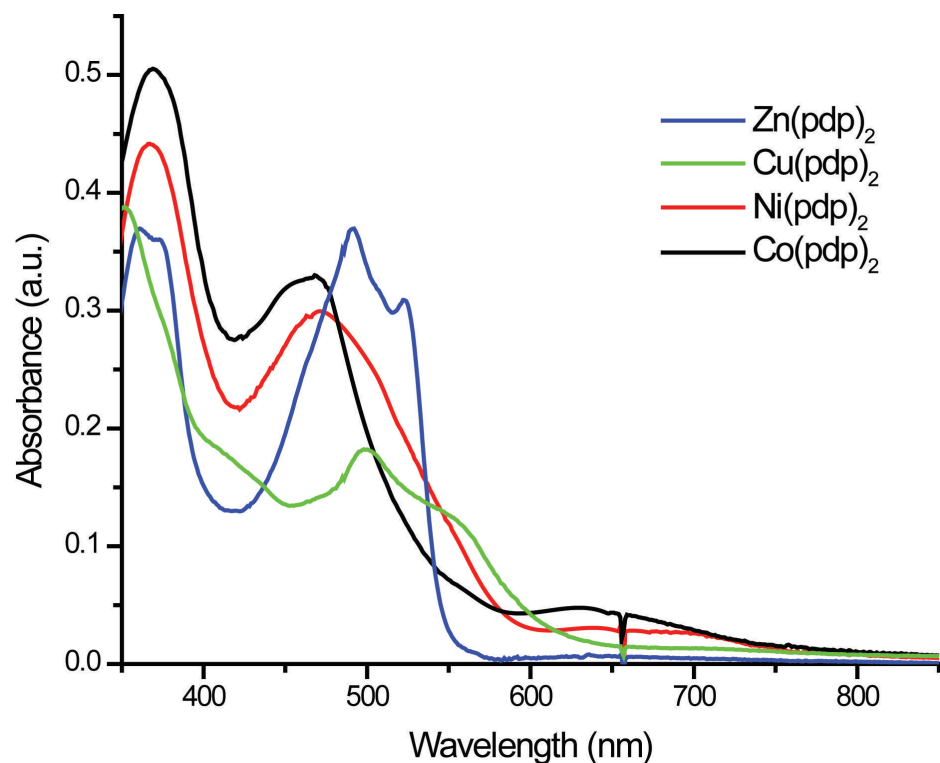


**Figure S3.** UV-visible absorption spectra of propentdyopent complexes (10-100 μM) in $CH_2Cl_2$.

***X-ray Diffraction Analysis.***

Data were collected at the University of Arizona Department of Chemistry and Biochemistry X-ray Diffraction Facility. Crystals were mounted onto a *MiTeGen* micromount under a protective film of Paratone® oil and diffraction data for all crystals were measured using a Bruker Kappa APEX II DUO diffractometer, with graphite-monochromated Mo-Kα radiation ($\lambda$ = 0.71073 Å) generated by a sealed tube, and an APEX II CCD area detector. The diffractometer was fitted with an Oxford Cryostream low-temperature device and data sets were collected using the *APEX2* software package (Bruker AXS Inc., Madison, WI, 2007). The data were corrected for absorption effects using a multi-scan method in *SADABS* (Sheldrick, G. M. University of Göttingen, Germany 1997). Experimental details of the

structure determinations are given in Table S2. All structures were solved by direct methods (*SHELXS-97*), and developed by full least-squares refinement based upon F$^2$ (*SHELXL*)[6] interfaced *via X-Seed*[7] and *OLEX2*.[8]

*Structure refinement of Zn(pdp)$_2$.* Crystals grew as bright orange needles by slow evaporation from a benzene solution at 5 °C. Data were collected, solved and refined in the triclinic space group P-1. The asymmetric unit was found to contain one complex molecule and half a benzene molecule. All wholly occupied non-H atoms were located in the Fourier map and refined anisotropically. H atoms were placed in calculated positions with fixed $U_{iso}$ at 1.2 times for all CH and CH$_2$ groups and fixed $U_{iso}$ at 1.5 times for all CH$_3$ groups, then their positions were refined using a riding model. No restraints or constraints were used in the final model. The model was found to be disordered at the methyl group centred at C(17) therefore this group was modelled over two positions with occupancy of 41% and 59%, offering a stable refinement. The highest residual Fourier peak found in the model was +0.41 *e*.Å$^{-3}$ approx. 0.71 Å from H10A and the deepest Fourier hole was found to be -0.31 *e*.Å$^{-3}$ approx. 0.65 Å from Zn1.

*Structure refinement of Cu(pdp)$_2$.* Dark red crystals were obtained by slow evaporation of CHCl$_3$ at 4 °C. The crystal employed for data collection was non-merohedrally twinned, and the structure was refined using a HKLF5 file containing data for two twin domains. No restraints were required in the model. The twin law, [-0.215 0.659 0.559 0.783 -0.343 0.558 0.784 0.658 -0.442], corresponding to a rotation of 180.0° about the reciprocal axis (1 1 1) was determined using *CELL_NOW* (Bruker AXS, 2009). Integration and absorption correction using TWINABS-2008/4 (Bruker 2010) gave 3750 unique reflections in domain 1, 3738 unique reflections in domain 2, and 4078 unique overlapping reflections. The structure was solved using the non-overlapping reflections from both domains (HKLF 4) and refined using corrected reflections from only the major component including overlaps (HKLF 5).

Data were collected, solved and refined as a 2-component perfect twin in the triclinic space group P-1. After transformation to P-1, the asymmetric unit was shown to contain one complete complex molecule and 2 chloroform molecules. All non-H atoms were located in the Fourier map and refined anisotropically while all H atoms, were placed in calculated positions with fixed $U_{iso}$ at 1.2 times for all CH and CH$_2$ groups and fixed $U_{iso}$ at 1.5 times for all CH$_3$ groups. Their positions were then refined using a riding model. The highest residual Fourier peak was +0.73 *e*.Å$^{-3}$ approx. 1.19 Å from Cu1. The deepest Fourier hole was found to be -0.54 *e*.Å$^{-3}$ approx. 0.51 Å from Cl(4).

*Note* – Single crystals of Cu(pdp)$_2$ (CCDC Refcode LEGBII) were previously obtained from the degradation of a copper complex of octaethylbilindione (*J. Am. Chem. Soc.*, 1993, **115**, 12206). The structure is a different solvate and was refined in a different space group; nevertheless, the connectivity and metrics of the complex indicate that the same species was isolated.

*Structure refinement of Ni(pdp)$_2$.* Brick-red crystals were obtained by slow evaporation of CDCl$_3$ at 4 °C. The analyzed single crystal was non-merohedrally twinned. The twin law, [-0.220  0.586  0.633 0.781 -0.413  0.632 0.779  0.588 -0.367], corresponding to a rotation of 180.0° about the reciprocal axis (1 1 1) was determined using CELL_NOW (Bruker AXS, 2009). Integration and absorption correction using TWINABS-2008/4 (Bruker 2010) gave 5000 unique reflections in domain 1, 4974 unique reflections in domain 2, and 3856 unique overlapping reflections. The structure was solved using the non-overlapping reflections from both domains (HKLF 4) and refined using corrected reflections from only the major component including overlaps (HKLF 4).

Data were collected, solved and refined as a 2-component perfect twin in the triclinic space group P-1. No restraints were required in the model. The asymmetric unit was shown to contain one complete complex molecule and 2 $CDCl_3$ molecules. The model was found to be disordered at the $CDCl_3$ solvent with carbon centered at C(6), therefore each chlorine atom of this group was modelled over two positions with occupancy of 44% and 56%, offering a stable refinement. All non-H atoms were located in the Fourier map and refined anisotropically while all H atoms, were placed in calculated positions with fixed $U_{iso}$ at 1.2 times for all CH and $CH_2$ groups and fixed $U_{iso}$ at 1.5 times for all $CH_3$ groups. Their positions were then refined using a riding model. The highest residual Fourier peak was +0.89 e.Å-3 approx. 0.88 Å from Cl5. The deepest Fourier hole was found to be -0.69 e.Å-3 approx. 0.84 Å from Cl4.

*Structure refinement of Co(pdp)₂.* Dark red needles were obtained by slow diffusion of benzene in a solution in $CH_2Cl_2$ at 4 °C Data were collected, solved and refined in the monoclinic space group C2/c. The asymmetric unit contains 0.5 complex molecule with two-fold symmetry and 0.5 dichloromethane molecule. All wholly occupied non-H atoms were located in the Fourier map and refined anisotropically. H atoms were placed in calculated positions with fixed $U_{iso}$ at 1.2 times for all CH and $CH_2$ groups and fixed $U_{iso}$ at 1.5 times for all $CH_3$ then their positions refined using a riding model. Co1 and C18 lie on special positions. Appropriate constraints were applied to coordinates and anisotropic thermal parameters. The model was found to be disordered at the two chlorine atoms of the dichloromethane molecule. The highest residual Fourier peak was +0.48 $e$.Å$^{-3}$ approx. 0.74 Å from Cl1 of the solvent dichloromethane molecule. This is likely due to disorder in the molecule, which could not be modeled. The deepest Fourier hole was found to be -0.51 $e$.Å$^{-3}$ approx. 0.84 Å from Cl1A.

*Note* – Single crystals of Co(pdp)₂ (CCDC Refcode PURXUV) were previously obtained from the degradation of a cobalt complex of octaethylbilindione (*Inorg. Chem.,* 1998, *37, 982*). Both structures present a dichloromethane solvent molecule and were refined in the monoclinic space group C2/c. In the present structure, anisotropic thermal parameters were refined for all non-hydrogen atoms, and hydrogen atoms were visible on the difference Fourier map. The refinement resulted in lower errors in atomic positional parameters for the new structure, which is reported herein for consistency of comparisons across the presented series of complexes (see Tables S3 and S4).

**Table S2.** Crystal data collection parameters

| | Zn(pdp)$_2$ | Cu(pdp)$_2$ | Ni(pdp)$_2$ | Co(pdp)$_2$ |
|---|---|---|---|---|
| Molecular formula | C$_{37}$H$_{44}$N$_4$O$_4$Zn | C$_{36}$H$_{44}$N$_4$O$_4$CuCl$_6$ | C$_{36}$H$_{42}$N$_4$O$_4$Cl$_6$NiD$_2$ | C$_{35}$H$_{44}$Cl$_2$CoN$_4$O$_4$ |
| Formula weight [g.mol$^{-1}$] | 674.13 | 872.99 | 870.17 | 714.57 |
| Temperature [K] | 100.0 | 120.0 | 99.7 | 150.0 |
| Crystal class | triclinic | triclinic | triclinic | monoclinic |
| Space group | P-1 | P-1 | P-1 | C2/c |
| a [Å] | 11.175(3) | 11.6428(10) | 12.2982(7) | 17.3525(11) |
| b [Å] | 11.683(3) | 13.6677(12) | 14.0284(7) | 13.8340(9) |
| c [Å] | 14.705(3) | 14.1795(12) | 14.0382(8) | 14.8976(9) |
| α [°] | 92.050(5) | 84.481(3) | 76.426(2) | 90 |
| β [°] | 105.445(5) | 68.110(2) | 67.944(2) | 102.894(3) |
| γ [°] | 110.322(6) | 72.003(3) | 64.685(2) | 90 |
| Volume [Å$^3$] | 1717.8(7) | 1990.8(3) | 2021.2(2) | 3486.1(4) |
| Z | 2 | 2 | 2 | 4 |
| $\rho_{calc}$ [g/cm$^3$] | 1.303 | 1.456 | 1.430 | 1.362 |
| $m$ [mm$^{-1}$] | 0.759 | 0.994 | 0.919 | 0.689 |
| F(000) | 712.0 | 902.0 | 900.0 | 1500.0 |
| Crystal size [mm] | 0.38 × 0.14 × 0.11 | 0.474 × 0.186 × 0.092 | 0.10 × 0.02 × 0.01 | 0.48 × 0.16 × 0.11 |
| Measured reflections | 29344 | 7563 | 7669 | 16182 |
| Independent reflections, $I > 2\sigma[I]$ | 6063 | 7563 | 7669 | 3074 |
| $R_{int}$ | 0.0560 | 0.0552 | 0.0656 | 0.0672 |
| Goodness-of-fit on F$^2$ | 1.011 | 1.086 | 1.054 | 1.034 |
| $R_1$, $I > 2\sigma[I]$[a] | $R_1$ = 0.0379, wR$_2$ = 0.0728 | $R_1$ = 0.0556, wR$_2$ = 0.1305 | $R_1$ = 0.0503, wR$_2$ = 0.1010 | $R_1$ = 0.0476, wR$_2$ = 0.1055 |
| $wR_2$, all data[b] | $R_1$ = 0.0638, wR$_2$ = 0.0810 | $R_1$ = 0.1004, wR$_2$ = 0.1516 | $R_1$ = 0.0849, wR$_2$ = 0.1101 | $R_1$ = 0.0755, wR$_2$ = 0.1160 |
| peak/hole [e Å$^{-3}$] | 0.41/-0.31 | 0.73/-0.54 | 0.89/-0.69 | 0.48/-0.51 |
| CCDC Number | 1431605 | 1431584 | 1434496 | 1434495 |
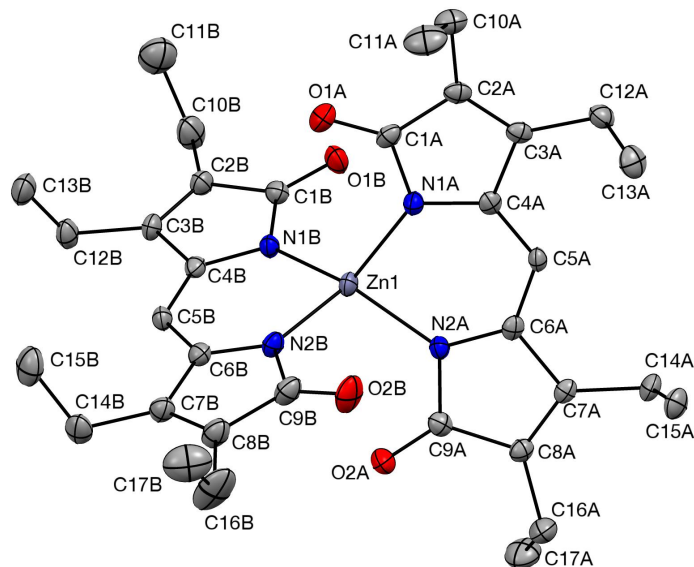
**Figure S4.** Crystal structure of Zn(pdp)$_2$ showing the full labeling scheme. Atoms are displayed as thermal ellipsoids at 50% probability. All hydrogen atoms, as well as a benzene molecule, were omitted for clarity. The same labeling scheme was employed for complexes Cu(pdp)$_2$ and Ni(pdp)$_2$. For the Co(pdp)$_2$ complex, in which Co1 lies on a center of symmetry, a single set of labels was required for the two equivalent pdp⁻ ligands.

**Table S3.** Comparison of selected bond lengths (Å) in the crystal structures of the propentdyopent complexes.

|  | Zn(pdp)$_2$ | Cu(pdp)$_2$ | Ni(pdp)$_2$ | Co(pdp)$_2$ |
|---|---|---|---|---|
| M1−N1A | 1.981(2) | 1.949(4) | 1.959(4) | 1.977(2) |
| M1−N2A | 2.002(2) | 1.966(4) | 1.957(4) | 1.968(2) |
| N1A-C1A | 1.406(3) | 1.409(7) | 1.420(7) | 1.399(4) |
| N1A-C4A | 1.345(3) | 1.353(6) | 1.349(7) | 1.349(4) |
| N2A-C6A | 1.352(3) | 1.348(6) | 1.349(7) | 1.350(4) |
| N2A-C9A | 1.411(3) | 1.404(7) | 1.415(7) | 1.400(4) |
| O1A-C1A | 1.214(3) | 1.215(6) | 1.210(6) | 1.216(4) |
| O2A-C9A | 1.213(3) | 1.232(6) | 1.209(7) | 1.212(4) |
| C1A-C2A | 1.499(4) | 1.485(7) | 1.504(8) | 1.501(4) |
| C2A-C3A | 1.340(3) | 1.335(8) | 1.344(8) | 1.331(4) |
| C3A-C4A | 1.507(4) | 1.490(7) | 1.491(7) | 1.489(4) |
| C4A-C5A | 1.392(3) | 1.389(7) | 1.387(7) | 1.391(4) |
| C5A-C6A | 1.392(3) | 1.391(7) | 1.391(7) | 1.384(4) |
| C6A-C7A | 1.495(3) | 1.494(7) | 1.492(7) | 1.494(4) |
| C7A-C8A | 1.342(3) | 1.334(7) | 1.344(8) | 1.326(4) |
| C8A-C9A | 1.502(3) | 1.497(8) | 1.499(7) | 1.510(4) |

**Table S4.** Comparison of selected angles (°) in the crystal structures of the propentdyopent complexes.

|  | Zn(pdp)$_2$ | Cu(pdp)$_2$ | Ni(pdp)$_2$ | Co(pdp)$_2$ |
|---|---|---|---|---|
| Dihedral angle | 79.8(1) | 54.0(2) | 69.8(1) | 73.5(1) |
| N1A−M−N2A | 91.94(8) | 91.34(17) | 89.81(10) | 91.95(10) |
| N1B−M−N2B | 92.53(8) | 90.94(18) | 89.73(10) | 91.94(10) |
| N1A−M−N1B | 114.47(8) | 99.99(17) | 107.31(10) | 129.13(15) |
| N1A−M−N2B | 123.85(9) | 144.67(17) | 124.11(10) | 109.64(10) |
| N2A−M−N1B | 125.95(9) | 139.72(17) | 141.84(11) | 109.64(10) |
| N2A−M−N2B | 111.22(8) | 101.80(17) | 108.84(10) | 128.97(15) |

**Electrochemical Measurements.** Cyclic voltammograms (CV) were carried out on a Gamry Reference 600 potentiostat employing a single-compartment cell and a three-electrode setup comprising a glassy carbon working electrode, a coiled platinum wire auxiliary electrode and Ag/AgCl pseudo-reference electrode. Measurements were conducted at ambient temperature under an argon atmosphere in CH$_2$Cl$_2$ containing 0.1 M ($n$-Bu$_4$N)(PF$_6$) (triply recrystallized) as an auxiliary electrolyte. Sample concentrations were 1−2 mM. All electrochemical data were referenced to the ferrocene/ferrocenium couple at 0.00 V.

For the spectroelectrochemical measurements, a three-electrode electrochemical quartz cell with a 1.0-mm path length (BASi EF-1358) was used with a Pt gauze working electrode (BASi EF-1355), a Ag wire (0.5 mm dia.) quasi-reference electrode housed in a glass tube (5.4 cm × 5.7 mm) with a Porous CoralPor™ Tip, and a Pt wire (1.0 mm dia.) as the counter electrode (BASi EF-1356). A stock solution of Zn(pdp)$_2$ (67 µM) was prepared in DMF containing 0.1 M ($n$-Bu$_4$N)(PF$_6$). All solutions were degassed with argon for ten minutes prior to experimentation and maintained under argon during electrolysis. For analysis, a linear sweep scan was carried out between –0.91 V to –2.71 V (vs Fc/Fc$^+$) in order to determine the potentials to be applied for electrolysis (Figure S5). A fresh aliquot from the stock solution was used for controlled potential electrolysis (Figure 3, main text). UV-visible absorption data acquisition was continued until saturation was reached: 200 s for the one-electron reduction at −1.2 V, and 400 s for the two-electron reduction at −1.8 V.

**Table S5.** Electrochemical data for the propentdyopent complexes

|  | Zn(pdp)$_2$ | Cu(pdp)$_2$ | Ni(pdp)$_2$ | Co(pdp)$_2$ |
|---|---|---|---|---|
| $E_{1/2}$[a] vs Fc/Fc+ ($\Delta E$) / V | −1.36 (86) | −1.39 (78) | −1.34 (94) | −1.33 (69) |
|  | −1.16 (84) | −1.13 (82) | −1.16 (93) | −1.14 (78) |
|  |  | 0.93 (82) | 0.74 (94) | $E_{cathodic}$= −0.23 |
|  |  |  |  | $E_{anodic}$= 0.68 |

[a] Half-wave potentials measured by cyclic voltammetry at a glassy carbon electrode in CH$_2$Cl$_2$ with ($n$-Bu$_4$N)(PF$_6$) as a supporting electrolyte. Data were collected at a 100 mV s$^{-1}$ scan rate, using a Ag/AgCl quasi-reference electrode and a platinum wire auxiliary electrode.
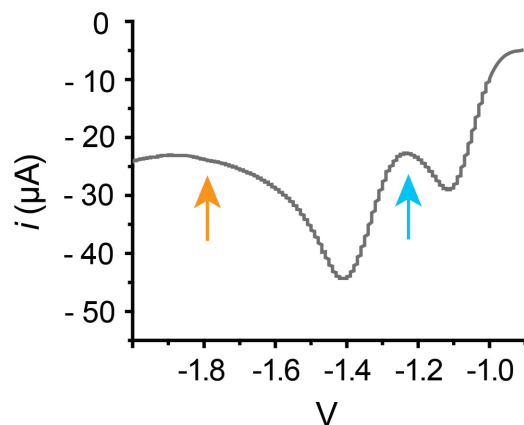
**Figure S5.** Linear sweep voltammogram (scan rate, 10 mV s$^{-1}$) showing the potentials selected for one-electron reduction (−1.2 V) and two-electron reduction (−1.80 V) in controlled potential electrolysis experiments.
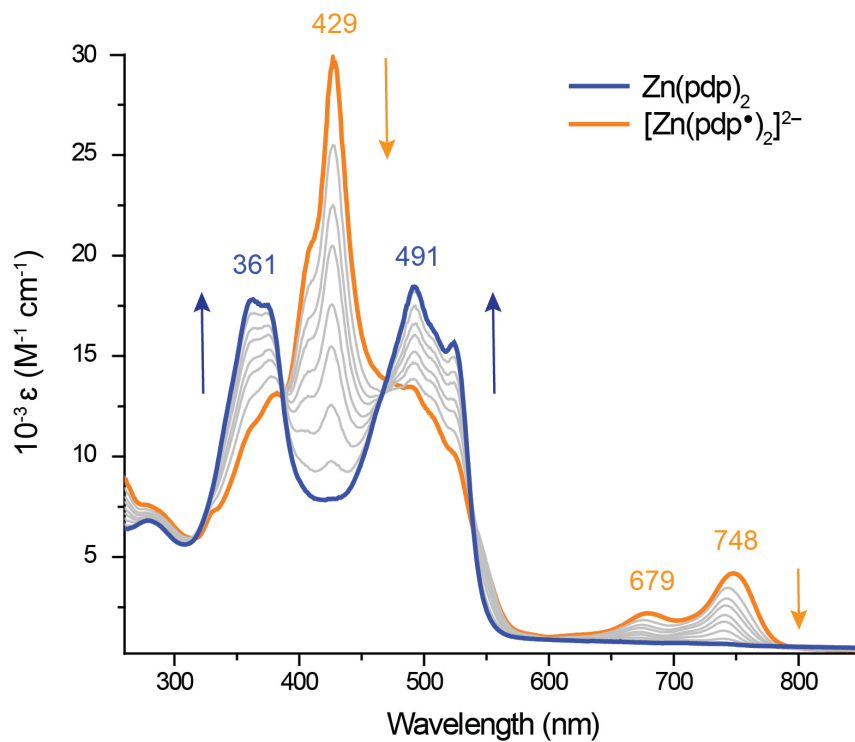


**Figure S6.** UV-visible spectral changes observed over a period of 4 minutes upon exposure to air of [Zn(pdp•)$_2$]$^{2-}$ (electrochemically generated, Figure 3) to yield the parent complex Zn(pdp)$_2$ quantitatively.

**EPR Measurements.** The continuous-wave (CW) EPR experiments were carried out at the University of Arizona EPR Facility on an X-band EPR spectrometer Elexsys E500 (Bruker) equipped with an ESR900 flow cryostat (Oxford instruments).

For the chemical reduction of $Zn(pdp)_2$, the complex (0.4−0.6 mM) was dissolved in THF under a nitrogen atmosphere in a glove box. Na(Hg) (5 wt % Na; 0.9−10.0 equiv.) was added and the reaction mixture was allowed to stir at room temperature. Samples for EPR measurements were collected from the reaction mixture at various time intervals, transferred to EPR tubes and frozen to perform measurements at low temperature (77 K).
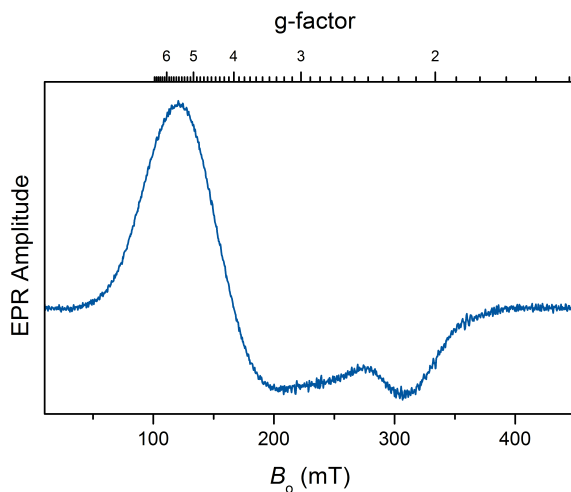


**Figure S7.** Frozen solution EPR spectrum of $Co^{II}(pdp)_2$ in a $CH_2Cl_2$/toluene mixture (1:1 v/v; toluene added for glassification). Experimental conditions: microwave (mw) frequency, 9.340 GHz; mw power, 20 mW; magnetic field modulation amplitude, 0.5 mT; temperature, 10 K. The principal g-values, $(g\perp, g_{\parallel}) \approx (4.5, 2.2)$, are close to those observed in other high-spin Co(II) complexes.[9, 10]
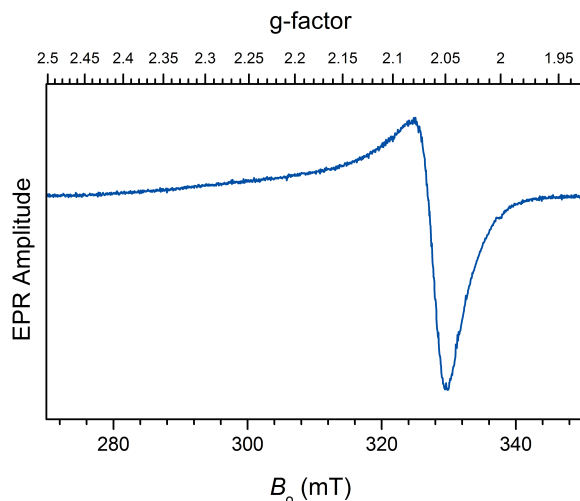
**Figure S8.** Frozen solution EPR spectrum of $Cu^{II}(pdp)_2$ in a $CH_2Cl_2$/toluene mixture (1:1 v/v). Experimental conditions: mw frequency, 9.455 GHz; mw power, 2 mW; magnetic field modulation amplitude, 0.5 mT; temperature, 77 K. No hyperfine structure due to $^{63,65}Cu$ nuclei is observed at the low-field region of the EPR spectrum because both the $^{63,65}Cu$ hyperfine interactions (*hfi*) and the principal g-values are distributed in broad limits. This distribution is caused by structural disorder related to a variation of the angle between the pdp ligand planes, C5A-Cu-C5B angle, and N-Cu-N angles.[11] The estimated mean principal g-values are: ($g\perp$, $g_{\parallel}$) ≈ (2.065, 2.245). The former ($g\perp$) corresponds to the zero crossing at $B_o$ ≈ 327 mT. The latter ($g_{\parallel}$) is estimated from $g\perp$ and the isotropic g-value ($g_{iso}$ ≈ 2.125) found from the EPR spectrum recorded for liquid solution at room temperature (shown in Fig. S9).
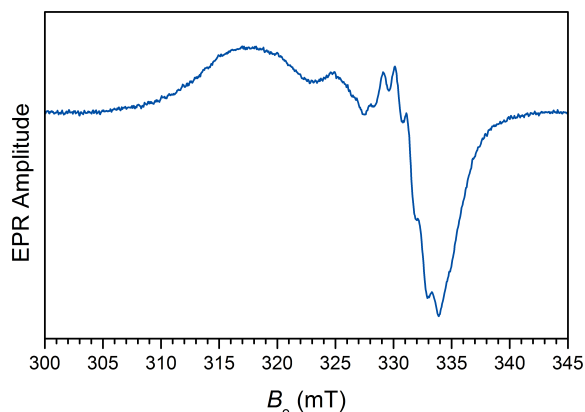


**Figure S9.** Liquid solution EPR spectrum of $Cu^{II}(pdp)_2$ in a $CH_2Cl_2$/toluene mixture (1:1 v/v). Experimental conditions: mw frequency, 9.638 GHz; mw power, 2 mW; magnetic field modulation amplitude, 0.5 mT; temperature, 298 K (room temperature). The isotropic principal g-value, $g_{iso}$ ≈ 2.125, corresponds to $B_o$ = 324 mT. The four broad lines caused by the *hfi* with the $^{63,65}Cu$ nucleus ($I = 3/2$) become progressively broader and smaller in amplitude toward the lower magnetic fields because of insufficiently fast rotation of the complex even at room temperature (the two low-field lines actually merge). The splitting between these major lines is $A_{Cu}$ ≈ 5.2 mT. The high-field line, which is broadened to the least extent, shows the resolved splittings due to the *hfi* of the ligand $^{14}N$ nuclei with $A_N$ ≈ 1.1 mT.

# References

1. Roth, S.D.; Shkindel, T.; Lightner, D.A. *Tetrahedron* **2007**, *63*, 11030–11039.
2. Bonnett, R.; Buckley, D.G.; Hamzetash, D. *J. Chem. Soc., Perkin Trans. 1* **1981**, 322-325.
3. Bonnett, R.; Ioannou, S.; Swanson, F. J. *J. Chem. Soc., Perkin Trans. 1* **1989**, 711-714.
4. Balch, A. L.; Mazzanti, M.; Noll, B. C.; Olmstead, M. M. *J. Am. Chem. Soc.* **1993**, *115*, 12206-12207.
5. Koerner, R.; Olmstead, M. M.; Van Calcar, P. M.; Winkler, K.; Balch, A. L. *Inorg. Chem.* **1998,** *37*, 982-988.
6. (a) G. M. Sheldrick, SHELXS97 and SHELXL97 Programs for Crystal Structure Solution and Refinement, University of Gottigen, Germany, **1997**; (b) Sheldrick, G. M. *Acta Crystallogr., Sect. A* **2008**, *64*, 112-122.
7. L. J. Barbour *J. Supramol. Chem.* **2001**, *1*, 189-191.
8. Dolomanov, O.V.; Bourhis, L.J.; Gildea, R.J.; Howard, J.A.K.;  Puschmann H. *J. Appl. Cryst.* **2008**, *42*, 339-341.
9. Horrocks, Jr., W. D.; Burlone, D. A. *J. Am. Chem. Soc.* **1976**, *98*, 6512-6516.
10. Krivokapic, I.; Zerara, M. ; Daku, M. L.; Vargas, A.; Enachescu, C.; Ambrus, C.; Tregenna-Piggott, P.; Amstutz, N.; Krausz, E.; Hauser, A. *Coord. Chem. Rev.* **2007**, *251*, 364–378.
11. Hoffmann, S. K.; Goslar, J. *J. Solid State Chem.* **1982**, *44*, 343-353.